Helically Wound Soft Actuators for Torsion Control*

Gina Olson[1] and Yiğit Mengüç[2]

***Abstract*— Individual soft actuators have been developed for elongation, contraction, bending and twist, but these actuators and their combinations have yet to demonstrate the range and flexibility of motion seen in common sources of biological inspiration, such as cephalopods. This paper presents a method for torsion control via sets of opposing contracting actuators wound helically around a cylindrical structure. By shortening one set of actuators, twist is developed, similar to the oblique muscles within octopus arms. The addition of helical actuators to systems with longitudinal and transverse actuators will enable control over orientation of the arm and antagonistic stiffening. A geometric model is used to quantify best-case developed twist, representing application to a constant dimension cylinder. This model is validated experimentally using a cable-driven prototype on a rigid cylinder with no torsional stiffness. To evaluate the interaction with a system of actuators, a mechanics model of the torsion actuators wrapped around a deformable center is proposed. This model is used to extend the solution given by W.M. Kier [*Zoological Journal of the Linnean Society*, Vol. 83, No. 4, 307-324, 1985], and shows that while significant twist can be lost to deformations of the internal structure, those with a Poisson's ratio approaching $\nu = 0.5$ mitigate this loss. Finally, the feasibility of the concept is demonstrated with McKibben actuators wound around foam.**

I. INTRODUCTION

Soft actuators, whether alone or as a part of a system, have yet to achieve the dynamic capabilities of biological analogs like cephalopod arms. Whether pneumatically powered, electroactive, or cable-driven, these actuators have individually shown the ability to elongate, contract, bend, and twist – motions that are dictated by the organization of elements within them, and are not commonly actively reconfigurable. Biological systems, in contrast, use simple – and similar – constituents to form complex systems capable of combined motions and dynamic forces beyond those of the original components.

Cephalopod arms and tentacles are composed of groups of muscles oriented in three directions: oblique (or helical), transverse, and longitudinal. Each muscle group can contract actively, extend passively, and maintains an approximately constant volume at physiological pressures. Kier determined that the tentacles' extraordinary range of motion and control over orientation comes from their morphology: the noted muscle groups actuate together and against each other to affect motion [1], [2]. Consider the example of the squid tentacle in Figure 1 [1]. The longitudinal muscles contract directly, while the transverse muscles tighten their cross section to force extension. Bending is created by joint activation of transverse and longitudinal muscles. Torsion is controlled by the helical muscles that wrap in both directions around the outside. The exact arrangement and size of each

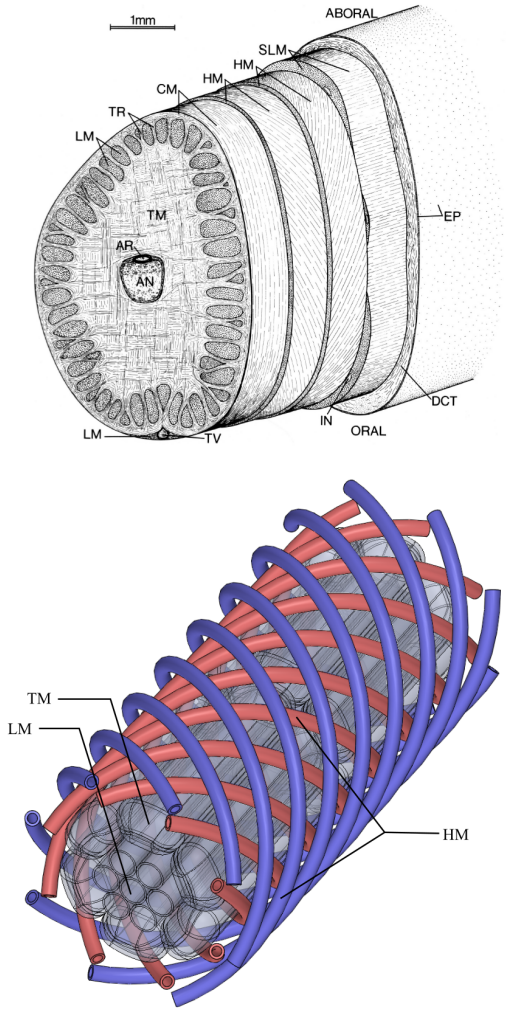

Fig. 1. Diagram of a left tentacular stalk of a loliginid squid [1], above, and a depiction of the helically wound actuator concept, below, around a possible soft robotic arm. In the upper, LM and SLM indicate longitudinal muscles, while CM, TR and TM indicate transverse muscles. HM indicates helical or oblique muscles, which are present in opposing pairs. The remaining indications are non-muscular anatomical features, such as connective and nervous tissue. In the lower, HM indicates the helically wrapped actuators studied here. LM and TM represent a possible system of soft actuators to create other motions, but are not studied here.

*This work was supported by the National Science Foundation, under award IIS-1734627.

[1]G. Olson is a Graduate Student in mLab at Oregon State University's Collaborative Robotics and Intelligent Systems Institute (e-mail: olsongi@oregonstate.edu).

[2]Y. Mengüç is mLab's Lab Director and an Assistant Professor at Oregon State University's Collaborative Robotics and Intelligent Systems Institute (e-mail: yigit.menguc@oregonstate.edu).

muscle group has been shown to vary by creature (e.g. elephant trunk, octopus arm, cuttlefish tentacle) and even by arm or tentacle within the same creature, according to their biological requirements [1].

Previous attempts to replicate the abilities of cephalopods, though numerous, have achieved only a subset of nature's capabilities. A simple approach is a tentacle that uses cables to drive bending and shortening, in a loose replication of longitudinal muscles [3]. A more common approach is to place in parallel three lines of extensile actuators, generating bending, and in some cases extension, by selectively activating actuator lines. This approach is used in Festo's Bionic Handling Assistant [4], in a serial pneumatic actuator arm developed in [5] and in the OCTARM developed in [6]. In both the Bionic Handling Assistant and OCTARM, though, the orientation of the gripper is controlled through a rigid rotary mechanism. Of those listed here, only the sPAM arm, which does not extend or twist, is completely soft.

Fewer systems have analogs to two or all three muscle groups. In [7] - [8], shape memory alloy actuators were connected to a braided structure to transform contraction into extension, while in [9] and [10], the transverse muscles were mimicked by pneumatic actuators placed orthogonally. All three muscle groups are replicated in [11] (though extension is not demonstrated), including bio-inspired soft torsional actuators, but the work does not examine actuator placement, geometry, expected performance or system interaction.

Soft actuator systems suffer the same limitations in robots not inspired by cephalopods. A variable stiffness gripper was developed using parallel actuators in [12], but it lacks independent orientation control. In [13] individual fiber-reinforced actuators, including a torsional actuator, were examined for serial combination, but this method has an inherently low mechanical advantage. In [14], helical actuators were antagonistically activated for joint stiffness modulation, but were not examined for torsion control.

This paper proposes a method of twist actuation and torsional stiffening directly inspired by the oblique muscles of cephalopod arms and investigates the interaction with a system of soft actuators. Current literature neglects soft twist actuation or focuses on individual fiber-reinforced actuators with limited twist and torque. The closest work, [11], does not explore system morphology. This paper examines the benefits and requirements of torsion actuators and presents the concept in Section II. The mathematical foundations of helically wound actuators around a constant dimension cylinder are presented as a geometric model in Section III, which is used to quantify best case performance. A mechanics model is then developed to explore the interaction between helical actuators and a deformable internal media, such as other soft actuators. This model is used to extend a solution presented by Kier that neglects twist [2]. Two prototypes are developed in Section IV. The first implements the concept with cables around a rigid cylinder and is used to validate the geometric model. In the second a pneumatic actuator is wound around foam to demonstrate concept feasibility in soft systems. The paper is concluded in Section V.

II. CONCEPT AND REQUIREMENTS OF TORSIONAL MUSCLES

Twisting actuators on a soft robot arm provide orientation control. The orientation of the distal tip can be controlled with two opposing helical actuators, while opposing actuators in series allow continuum control. Suckers on cephalopod arms cover only part of the exterior surface, so torsion control is required to orient them to the target. Antagonistic activation increases the torsional stiffness of the arm, improving the ability of capturing tentacles to restrain prey [1]. Twist can be developed in an individual pneumatic actuator wrapped by an inextensible fiber, and it can be combined with bending by wrapping two inextensible fibers at different angles [15], [16]. However, these actuators are difficult to integrate into systems, and lack mechanical advantage. Our identified requirements and concept are presented to address these challenges.

A. Requirements of Torsional Muscles

When used alone, torsional actuators must twist with enough torque to move themselves and the desired load. When used in conjunction with other actuators, the system imposes additional requirements. Though not comprehensive, the following are proposed to frame further examination of the concept:

- *Develop the desired twist.* For an end effector to have a complete orientation range, only 180° of twist in each direction is required. However, tasks like matching sucker position to objects could require more than 180° of twist in a given direction. This concept's twist performance is examined in depth in this paper.
- *Generate enough torque to overcome system stiffness and carry the desired load.* The actuator torque is specific to the type and design, but multiple actuators could be placed in parallel for a higher total. The actuators are expected to gain mechanical advantage from exterior placement, and to modulate stiffness, as in [14]. This is not examined in detail in this work.
- *Allow other motions.* In a complete arm, the torsional actuators must be compliant enough to allow contraction, elongation and bending. Helical structures can accommodate height change with little strain, and the demonstrations in [14] suggest they can also accommodate bending. This is not studied in detail in this work.

B. Concept Description

In this concept, two sets of contracting actuators are wound helically up a cylindrical structure – whether rigid or compliant - in opposite directions. This is a close replication of cephalopod arms (see Figure 1). The origin of paired actuators is identical and fixed, while the termination point is connected to the distal end of the structure or segment. When the actuators contract, they are assumed to maintain a helical shape and remain on the cylindrical surface. The number of turns in the active helix reduces as the length does, developing twist in the encapsulated structure in the direction of the contraction. This is illustrated in Figure 2.

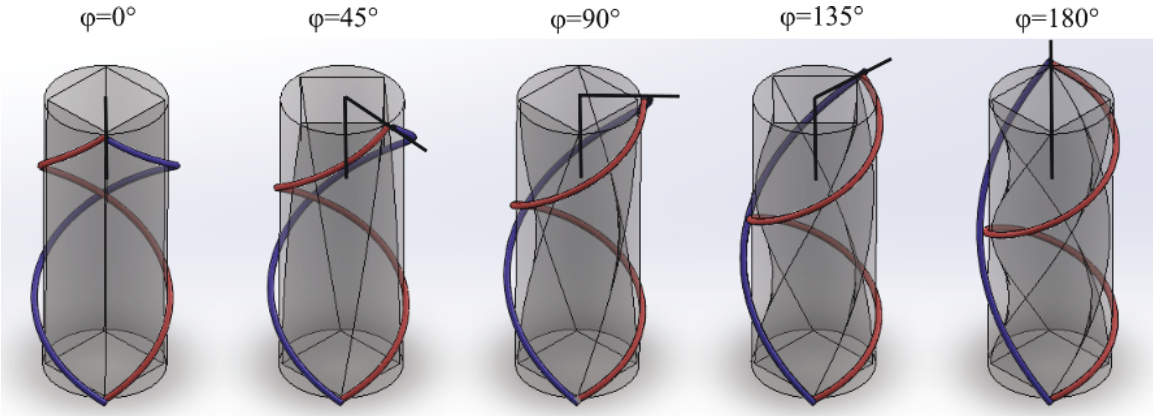

Fig. 2. Demonstration of helical actuators developing twist in a structure. The actuators start with one turn each. The blue actuator shortens, developing 45° of twist in the structure between each frame (denoted by ϕ). The red actuator passively lengthens to remain connected to the same termination point.

Though Figures 1 and 2 show the concept as though it were implemented with pneumatic actuators, a particular actuator is deliberately not selected. The concept is applicable to any contracting actuator, such as cables, McKibben actuators, or inverse pneumatic artificial muscles [17].

III. ANALYTICAL MODEL OF HELICAL ACTUATORS

While finite element models can provide high fidelity output (given high fidelity input), simpler (and less accurate) analytical models often provide more physical insight. Two models were developed to evaluate twist performance of helical actuators: a geometric model and a mechanics model.

The geometric model, given in Section III-A, assumes the internal cylinder to be of constant dimension. This idealized condition is more appropriate to traditional robotics, but it establishes a best-case performance, and the model can be used to explore the effect of varying helix parameters. This model relates contraction to twist, irrespective of materials.

The mechanics model, presented in Section III-B, allows the height and radius of the internal cylinder to change as it twists. The defining challenge of wholly soft actuator systems is their inherent compliance – unlike traditional robots, which can actuate without changing any dimensions other than the intended one, extension or contraction in soft arms can significantly change the cross-sectional dimensions and stiffness. The actuators within and connected to the structure must accommodate these changes, and their performance evaluated within that context. Though the internal structure is not known, the proposed solution models it as a set of springs with known stiffness. This technique allows the actuator groups to be modeled separately, while still examining their interconnectedness.

A. Geometric Model

Consider a single helix wound η times about a cylinder of height *h* and radius *r*, with parameters as defined in Figure 3. A helix is simply a straight line wrapped up the surface of the cylinder at a constant pitch, and so the length of the helix is the hypotenuse of the triangle formed by the cylinder height and length of the circumferential wrap. Helices may be fully described by three independent parameters, generally some combination of height, radius, angle, length and number of turns. In this case, it is initially convenient to define the length in terms of height, radius and number of turns, and solve for helix angle θ separately.

$$l = \sqrt{(2\pi r\eta)^2 + h^2} \tag{1}$$

$$\tan\theta = \frac{2\pi r\eta}{h} \tag{2}$$

Twist in the structure, as shown in Figure 2, is developed as the helix arc length shortens. To evaluate the amount of twist ϕ, the actuator is assumed to remain helical and bound to a cylindrical surface of constant height h_0 and radius r_0. In all cases, the subscript *0* refers to the initial configuration, c refers to the contracted configuration, and e refers to the elongated configuration. Contraction is defined in Eq. 3 as a ratio of lengths. The origin of the helix, at the base of the cylinder, is assumed to be fixed. The amount of twist, then, is given by the angular difference between the initial and final helix termination points, which can be written as a difference in the number of turns.

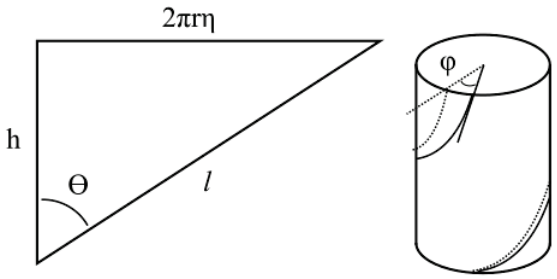

Fig. 3. Definition of helix parameters as they are used within this paper. The helix angle θ is defined from the longitudinal axis, while the height and radius are identical to that of the cylinder wrapped by the helix. The number of turns is given by η, and the developed twist by ϕ.

$$\alpha_c = \frac{l_c}{l_0} \tag{3}$$

$$\phi = 2\pi(\eta_0 - \eta_c) \tag{4}$$

Note η_c, the number of turns after contraction, is assumed to be less than η_0, and so Eq. 4 is written such that ϕ is positive. Eq. 1 can be rewritten for the contracted configuration, and Eq. 4 and Eq. 1 substituted to produce a relation between the initial helix parameters, the contraction ratio and the twist.

$$\alpha_c l_0 = \sqrt{(2\pi r_0 \eta_c)^2 + h_0^2} \tag{5}$$

$$\phi = 2\pi \left(\eta_0 - \frac{\sqrt{((2\pi r_0 \eta_0)^2 + h_0^2)\alpha_c^2 - h_0^2}}{2\pi r_0} \right) \tag{6}$$

This result can be simplified by redefining the helix in terms of the initial angle θ_0 and substituting, to produce a relationship between the developed twist, contraction and the initial helix angle and number of turns. The height and radius are then defined implicitly, but Eq. 7 can be rewritten in terms of a cylinder aspect ratio instead of the number of turns.

$$\phi = 2\pi\eta_0 \left(1 - \sqrt{\left(1 + \frac{1}{\tan^2\theta_0} \right) \alpha_c^2 - \frac{1}{\tan^2\theta_0}} \right) \tag{7}$$

$$\phi = \frac{h_0}{r_0} \left(\tan\theta_0 - \sqrt{\left(\tan^2\theta_0 + 1 \right) \alpha_c^2 - 1} \right) \tag{8}$$

Eq. 7 suggests that developed twist is nearly linear with contraction. The idealized behavior can be further explored using Eq. 7 and Eq. 8 by varying initial helix geometry. In Figure 4, helices are defined by the initial angle and number of turns, and the contraction required to produce 180° of twist, calculated from Eq. 7, is plotted.

The contraction required to reach 180° decreases for a given helix angle as the number of turns increases, while lower helix angles require less contraction to achieve the same twist. The first observation is explained by noting that the number of turns lost to produce 180° of twist is one half-turn regardless of the initial number of turns, so the ratio approaches unity as η increases. The second observation identifies a weakness in the model: it imposes a contraction regardless of whether it can be physically accomplished. At low helix angles, small length changes produce large twists, but the actuator force — directed along the helix — is nearly perpendicular to the desired direction of motion.

In Figure 5, the same exploration is done with helices defined by the cylinder aspect ratio. This solution can be more helpful in imagining an arm of a certain size wrapped at a particular angle. Because the number of turns is defined implicitly, it is possible for low angle helices to be too short to produce 180° of twist. The set of valid solutions can be found by writing an inequality between the cylinder height and the contracted arc length, as the helix length cannot shorten beyond the height. This gives the maximum valid contraction for a given initial helix angle (note: the contraction ratio decreases as amount of contraction increases).

$$l_0 \alpha_c > h_0 \tag{9}$$

$$\alpha_c > \cos\theta_0 \tag{10}$$

Figure 5 identifies two regions of good performance but practical challenges: very low helix angles, which misdirect the force, and very high helix angles, which require very long actuators. It also identifies, in the approximate middle of each curve, a set of solutions that require large contractions, suggesting the ideal solution may be in the first or fourth quartile.

An identical second helix, wound opposite to the first with the same origin and termination points, can be added to the

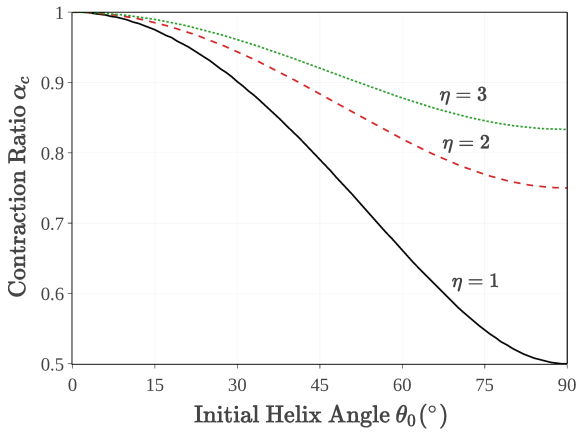

Fig. 4. The contraction ratio required to produce 180° of twist for a given initial helix angle, plotted for one, two and three turns (η) initially. Twisting 180° is equivalent to unwinding half a turn, so the higher the initial turns, the less contraction is needed at all angles to produce the same twist.

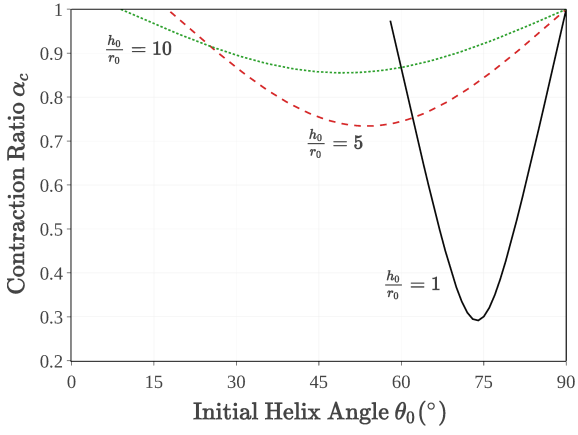

Fig. 5. The contraction ratio required to twist 180° for a given initial helix angle, plotted for three aspect ratios and truncated to include only valid solutions per Eq. 10. At low angles, small contractions produce large twists, while at high angles, the greater number of turns drives $\frac{\eta}{\eta_0}$ to one.

model. As the active helix contracts, the passive helix must extend. A similar approach can be taken to find the required extension, by assuming an expansion ratio α_e and relating the increased number of turns η_e to the previously determined twist ϕ.

$$\alpha_e = \frac{l_e}{l_0} \tag{11}$$

$$\eta_e = \eta_0 + \frac{\phi}{2\pi} \tag{12}$$

Note that η_e has been assumed to be greater than η_0, and Eq. 12 written to match the previously assumed sign of developed twist. Following the method presented previously and solving for α_e yields a result in terms of helix parameters.

$$\alpha_e = \sqrt{\alpha_c^2 + \frac{4\tan^2\theta_0}{\tan^2\theta_0 + 1}\left(1 - \sqrt{\alpha_c^2 + \frac{\alpha_c^2 - 1}{\tan^2\theta_0}}\right)} \tag{13}$$

The net length change in active contraction, then, is not necessarily equal to the net length change in passive extension (i.e. $\alpha_c = 0.75$, α_e is not guaranteed to be 1.25). Experimental results shown in Section IV suggest that as the number of turns increases, the length changes approach equality.

B. Mechanics Model

The weakness of the geometric model is that it ignores the mechanics of both the helical actuators and the internal cylinder. As the actuators contract, they tighten radially around the structure, and exert a torque and a downward force, with the fraction of the force to each dependent on the changing helix angle. For an encapsulated deformable cylinder, this could reasonably be expected to change its height and radius. In cephalopod arms, the muscles undergo drastic dimensional changes. Kier derived the relation in Eq. 14, with parameters as defined in Figure 6, to quantify the deformation of the arm when the oblique muscles were activated [2]. The volume *V* is constant, but by neglecting η, this solution presumes the number of turns to also be constant and singular, and thus no twist is developed.

$$D = \sqrt[3]{\frac{3\pi V}{\sin^2\theta\cos\theta}} \tag{14}$$

Once deformation and twist are allowed, the system cannot be fully defined geometrically. This was also noted by G. Krishnan, who found a deformable cylinder defined by a single helix was geometrically underconstrained [15]. As the helix shortens, the internal cylinder can shorten, widen or twist to resolve the length change. The inclusion of deformation in a model is complicated by the unknown internal structure. Selecting a particular structure would severely limit the applicability of the model, and prevent later co-optimization of actuator groups. Instead, a solution form is proposed from a combination of three equations: a geometric constraint, minimization of potential energy, and a third closing equation derived from system knowledge.

The solution is developed in three steps, ending in an extension of Kier's original solution. In every step a contraction α_c is imposed, and, and is presumed to generate a twist ϕ, a change in radius Δr, and a change in height Δh. Assuming that the internal cylinder remains cylindrical (thus assuming that no buckling occurs) and the actuators remains helical, Eq. 1 can be used to write a geometric constraint.

$$\alpha_c l_0 = \sqrt{\left(2\pi(r_0 - \Delta r)(\eta_0 - \frac{\phi}{2\pi})\right)^2 + (h_0 - \Delta h)^2} \tag{15}$$

The total potential energy of the deformable media will tend to a minimum, which can be used to relate the deformations. This approach is, in some ways, the inverse of the approach in [18], in which an energy model is used to determine load from deformation. To solve Eq. 16 as written, Δr and Δh must be described in terms of ϕ.

$$\frac{dE(\phi, \Delta r, \Delta h)}{d\phi} = 0 \tag{16}$$

First, consider a simpler case, where the height is fixed ($\Delta h = 0$). To solve Eq. 16, the system energy must

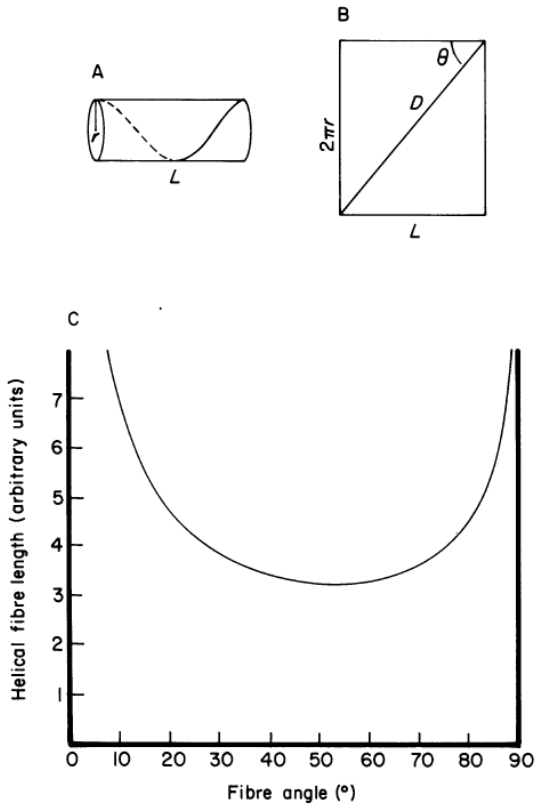

Fig. 6. Definition and result of oblique muscle model as presented by Kier, reproduced exactly from the original source [2]. Kier defines the length of the helix by cylinder radius and height, neglecting the number of turns and thus assuming it to be constant and singular. The solution assumes constant volume, and models the length and radius change of the oblique muscles without twist. This represents antagonistic activation.

be described in terms of the deformation. The cylindrical structure is therefore modeled as two springs: a radial spring, with stiffness k_r, and a torsion spring, with stiffness k_τ. In this work, both stiffnesses are assumed to be constant. The energy of the system can then be written as the sum of two spring energies, and solved with just the geometric constraint in Eq. 15.

$$E = \frac{1}{2}(k_r \Delta r^2 + k_\phi \phi^2) \tag{17}$$

$$\Delta r = r_0 - \frac{\sqrt{\alpha_c^2 l_0^2 - h_0^2}}{2\pi\eta_0 - \phi} \tag{18}$$

$$\frac{k_\tau}{k_r}\phi = \left(\frac{r_0\sqrt{\alpha_c^2 l_0^2 - h_0^2}}{(2\pi\eta_0 - \phi)^2} - \frac{\alpha_c^2 l_0^2 - h_0^2}{(2\pi\eta_0 - \phi)^3} \right) \tag{19}$$

To identify the effect of the ratio of torsional and radial stiffness, the result is plotted in Figure 7 for a sample helix, using the same contraction that produced 180° according to the geometric model. When the radial stiffness is high, the result approaches that of the geometric model. When the radial stiffness is low in comparison to the torsional stiffness, though, developed twist vanishes.

The solution can then be extended to allow height change. The spring model can be similarly extended to include a vertical spring with stiffness k_h, and Eq. 16 rewritten accordingly. This third deformation, though, requires a third constraining relation to solve. Most soft robotic systems are not truly constant volume, nor do many exhibit a constant Poisson's ratio. Initially, therefore, the system will be closed with a force and moment balance between the contracting actuator and the internal cylinder.

$$E = \frac{1}{2}(k_h \Delta h^2 + k_r \Delta r^2 + k_\tau \phi^2) \tag{20}$$

The actuator force is assumed to act down its length, and the vertical component of that force can be equated to the return force generated by the vertical spring. This introduces an actuator force F_a, an additional unknown. Assuming a force profile and applying that with the contraction would over-define the system, and thus a moment balance is used to equate spring torque to actuator torque.

$$F_a \cos\theta = k_h \Delta h \tag{21}$$

$$F_a \sin\theta (r_0 - \Delta r) = k_\tau \phi \tag{22}$$

Eq. 21 and 22 can then be solved to eliminate the actuator force, and be written in terms of height, radius and twist instead of helix angle.

$$\Delta h = \frac{h_0 k_\tau \phi}{k_\tau \phi + k_h (r - \Delta r)^2 (2\pi\eta_0 - \phi)} \tag{23}$$

The dependency between Δr and Δh creates an implicit relationship in both the geometric constraint and the energy minimization, so the system of equations was solved numerically. The results are plotted in Figure 8 against a varying vertical spring stiffness for two different sets of radial and torsional spring stiffnesses. The same sample helix used in Figure 7 was used for this study.

As the vertical spring stiffness increases, the result naturally approaches the solution in Eq. 19, where $\Delta h = 0$. However, when the internal cylinder is both radially and vertically compliant in comparison to torsional stiffness, twist again diminishes to almost nothing. Note two assumptions within this model: (1) though Δh and Δr are loosely interrelated, the structure may decrease size in both directions, which is representative of collapsing hollow structures, and (2) this model assumes constant stiffness for solution ease.

Using the above framework, the energy minimization approach can be used to extend Kier's derivation. The force and moment balance are replaced with a constant volume assumption, enforcing a Poisson's ratio of 0.5. Note that,

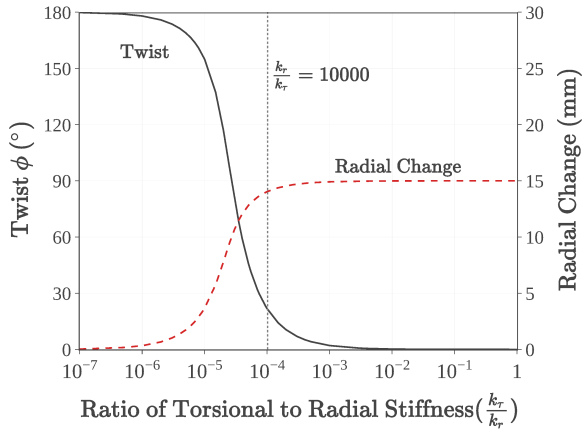

Fig. 7. Developed twist ϕ and radial change as the stiffness ratio $\frac{k_\tau}{k_r}$ varies, plotted against a logarithmic scale. This result is for a helix of initial height 150 mm, radius 30 mm, and single turn at angle 51.5°. The contraction ratio $\alpha_c = 0.74$, which produced 180° of twist in the geometric model.

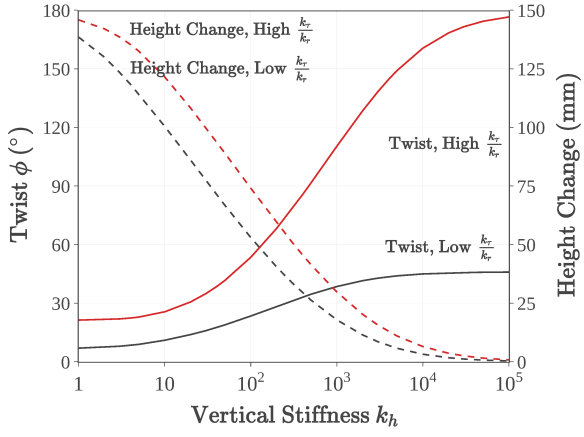

Fig. 8. Twist ϕ and height change as k_h varies, plotted against a logarithmic scale. Radius changes are omitted for figure clarity. This result is for the same sample helix used in Figure 7. Two cases are plotted: first, a ratio of $\frac{k_\tau}{k_r} = 5E-5$ and second, a ratio of $\frac{k_\tau}{k_r} = 5E-7$.

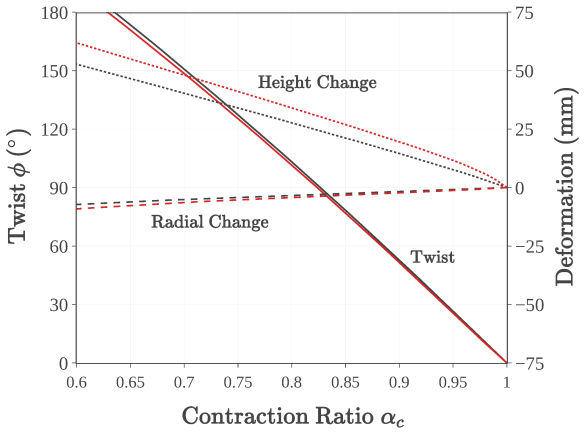

Fig. 9. Twist ϕ and change in radius and height as imposed contraction α_c varies. This result is plotted for the same sample helix used in Figure 7 and Figure 8. Two cases are plotted: first, a ratio of $\frac{k_\tau}{k_r} = 5E-5$ (black) and second, a ratio of $\frac{k_\tau}{k_r} = 5E-4$ (red). The vertical spring stiffness was $k_h = 0.5\frac{N}{m}$ in both cases.

despite this, all deformations are defined as decreases for notation consistency.

$$(r_0 - \Delta r)^2(h_0 - \Delta h) = r_0^2 h_0^2 \tag{24}$$

As before, the set of equations is solved numerically. The deformations for the sample helix are plotted in Figure 9, for two ratios of torsional to radial stiffness, though the vertical stiffness is constant between them.

The results show that, for compliant structures, significantly more twist is developed for a given contraction around a constant volume structure ($\nu = 0.5$) than around a structure with no Poisson's ratio. This is due to the inverse proportional relationship between Δh and Δr, which forces an increase in one dimension with the perpendicular dimension decreases. Note that even when the ratio between k_τ and k_r increased (which had previously greatly diminished twist), the change in developed twist was small.

IV. PROTOTYPE AND TESTING

To validate the concept and the geometric model, helical actuators were implemented with both cables and pneumatic actuators. The cable-driven actuator was used to validate the geometric model, while the pneumatic actuator was successfully used as a qualitative proof of concept.

A. Prototype Construction

The cable-driven prototype consists of a rigid cylinder with a rotary joint at the top, with cables wound in both directions. The rigidity of the model preserves the dimensions, while the rotary joint allows for twisting without significant torsional resistance. This implementation is shown in Figure 10.

In the pneumatic version, an actuator was wrapped around a cylindrical foam core, which serves as the deformable media. A single McKibben actuator was used, tied to 3D printed caps adhered to the foam. This implementation is shown in Figure 11.

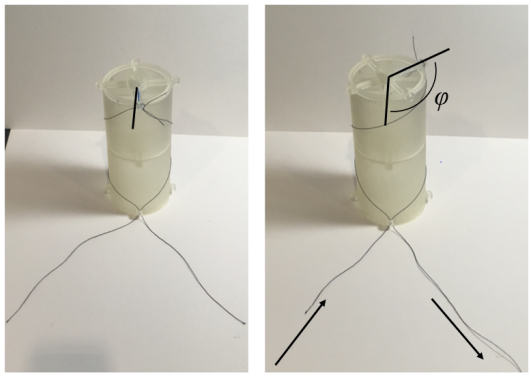

Fig. 10. A cable-driven rigid mechanism prototype, also used for the results in Figure 13. As the contracting side shortens, twist is developed, and the opposing helix lengthens. In this picture, the top has twisted $\sim 115°$.

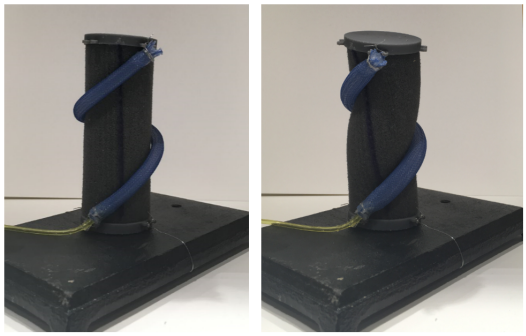

Fig. 11. A pneumatic prototype with a single McKibben actuator. As the actuator pressurizes and shortens, it places a concentrated load on the foam core. At maximum contraction, the core twisted $\sim 60°$.

Construction of the prototypes validated the need for the mechanics model, and demonstrated another challenge. The contraction of McKibben actuator changed the height of the foam, but as a tilt in the top, not a uniform decrease. The same concentrated loading was apparent radially as well, locally indenting the foam. This spot loading was a result of using only one actuator; a more distributed set of actuators might produce more even loading. This need for distributed forces may be one reason for the apparent redundancy in cephalopod arms.

B. Testing

The cable-driven prototype was also used to validate the geometric model, as it is constant dimension. Twist was measured via marks in the rotary joint, and the length of the contracting and extending cables were measured and compared to theory. The test set-up is shown in Figure 12.

The results for three initial helix angles are shown in Figure 13, though six were tested. In all cases the data was close to theory. The slight differences are likely due to measurement resolution and cable variation from a helix. Retaining a helical form is assumed in all presented models, but the experiment showed that low stiffness actuators with large numbers of turns drifted away due to gravity. However, even this produced little numerical error.

Fig. 12. Geometric model validation test set-up. The length change of the cables was measured with a ruler. Twist was measured via indentations in the rotary joint placed every 5° on both the base and top.

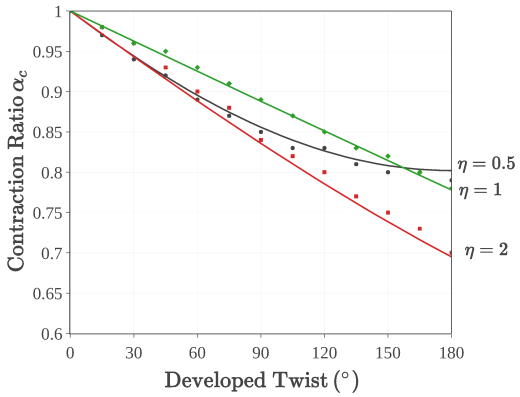

Fig. 13. Comparison between measured contraction (points) and theory (solid lines), plotted for three different initial number of turns.

V. CONCLUSIONS

This paper has presented and analyzed a biologically inspired method of torsion control via helically wound actuators, which exists as a gap in the literature today. Though commonly neglected or solved with traditional rotary joints, twisting actuators allow for control of end effector orientation and antagonistic stiffening. In octopuses, torsion control is required to orient suckers to targeted surfaces.

The presented models provide an analytical foundation for estimating twist performance alone and in a larger system. The geometric model gives a theoretical maximum twist, and has been validated for cylindrical structures with constant dimensions. The mechanics model connects the developed twist to the stiffness of an internal deformable media, and proposes a stiffness representation of internal actuator groups to allow for independent study and later co-optimization. The model finds that in unrestrained media the ratio of torsional stiffness to vertical and radial stiffness determines the amount of twist lost to other deformations, and predicts that twist will vanish in vertically and radially soft media. Internal media with a constant volume ($\nu = 0.5$), like cephalopod muscle, do not show this same sensitivity to stiffness ratios. This extends Kier's original torsion solution, which was valid only for deformation change due to antagonistic stiffening (no twist developed) [2]. This model could be used to design for combined twisting and extension or contraction, replicating nature's ability to use self-interference, which might otherwise be considered problematic, to produce complex motions.

This work has laid the foundations for a system integration with other actuators, and future work will focus on expanding the models to include more detailed stiffness representations, such as varying and interdependent spring stiffnesses. This model could then be validated with a distributed system of actuators, progressing towards a more capable soft robot arm.

REFERENCES

[1] W. Kier, "The musculature of coleoid cephalopod arms and tentacles," *Frontiers in Cell and Developmental Biology*, vol. 4, 2016.

[2] W. Kier and K. Smith, "Tongues, tentacles and trunks: the biomechanics of movement in muscular-hydrostats," *Zoological Journal of the Linnean Society*, vol. 83, no. 4, pp. 307–324, 1985.

[3] M. Calisti, M. Giorelli, G. Levy, B. Mazzolia, B. Hochner, C. Laschi, and P. Dario, "An octopus-bioinspired solution to movement and manipulation for soft robots," *Bioinspiration & Biomimetics*, vol. 6, no. 3, 2011.

[4] Festo, "Bionic handling assistant." https://www.festo.com/group/en/cms/10241.htm, 2017. Accessed 04 Dec 2017.

[5] J. Greer, T. Morimoto, A. Okamura, and E. Hawkes, "Series pneumatic artificial muscles (spams) and application to a soft continuum robot," *IEEE International Conference on Robotics and Automation (ICRA 2017)*, 2017.

[6] I. Walker, D. Dawson, T. Flash, F. Grasso, R. Hanlon, B. Hochner, W. Kier, C. Pagano, C. Rahn, and Q. Zhang, "Continuum robot arms inspired by cephalopods," *Proceedings SPIE Conference on Unmanned Ground Vehicle Technology VII*, pp. 303–314, 2005.

[7] M. Follador, M. Cianchetti, and C. Laschi, "Development of the functional unit of a completely soft octopus-like robotic arm," *4th IEEE RAS & EMBS International Conference on Biomedical Robotics and Biomechatronics (BioRob 2012)*, 2012.

[8] M. Cianchetti, M. Follador, B. Mazzolai, P. Dario, and C. Laschi, "Design and development of a soft robotic octopus arm exploiting embodied intelligence," *IEEE International Conference on Robotics and Automation (ICRA 2012)*, 2012.

[9] E. Guglielmino, N. Tsagarakis, and D. Caldwell, "An octopus anatomy-inspired robotic arm," *IEEE/RSJ International Conference on Intelligent Robots and Systems (IROS 2010)*, 2010.

[10] R. Kang, E. Guglielmino, L. Zullo, D. Branson, I. Godage, and D. Caldwell, "Embodiment design of soft continuum robots," *Advances in Mechanical Engineering*, vol. 8, no. 4, 2016.

[11] T. Doi, S. Wakimoto, K. Suzumori, and K. Mori, "Proposal of flexible robotic arm with thin mckibben actuators mimicking octopus arm structure," *IEEE/RSJ International Conference on Intelligent Robots and Systems (IROS 2016)*, pp. 5503–5508, 2016.

[12] L. A. Abeach, S. Nefti-Meziani, and S. Davis, "Design of a variable stiffness soft dexterous gripper," *Soft Robotics*, vol. 4, no. 3, pp. 274–284, 2017.

[13] F. Connolly, P. Polygerinos, C. Walsh, and K. Bertoldi, "Mechanical programming of soft actuators by varying fiber angle," *Soft Robotics*, vol. 2, no. 1, pp. 26–32, 2015.

[14] X. Zhang, G. Singh, and G. Krishnan, "A soft wearable sleeve for joint stiffness modulation," *IEEE International Conference on Advanced Intelligent Mechatronics (AIM 2016)*, 2016.

[15] G. Krishnan, J. Bishop-Moser, C. Kim, and S. Kota, "Kinematics of a generalized class of pneumatic artificial muscles," *Journal of Mechanisms and Robotics*, vol. 7, no. 4, 2015.

[16] W. Felt and C. Remy, "A closed-form kinematic model for fiber-reinforced elastomeric enclosures," *Journal of Mechanisms and Robotics*, vol. 10, no. 1, 2018.

[17] E. Hawkes, D. Christensen, and A. Okamura, "Design and implementation of a 300% strain soft artificial muscle," *IEEE International Conference on Robotics and Automation (ICRA 2016)*, 2016.

[18] A. Sedal, D. Bruder, J. Bishop-Moser, R. Vasudevan, and S. Kota, "A constitutive model for torsional loads on fluid-driven soft robots," *ASME International Design Engineering Technical Conferences and Computers and Information in Engineering Conference (IDETC/CIE 2017)*, 2017.